NANO EXPRESS

PAPER

Point Defects in InGaN/GaN Core–Shell Nanorods: Role of the Regrowth Interface

K Loeto[1], G Kusch[1], P-M Coulon[2], SM Fairclough[1], E Le Boulbar[2], I Girgel[2], PA Shields[2] and RA Oliver[1]

[1] Department of Materials Science and Metallurgy, University of Cambridge, CB3 0FS Cambridge, United Kingdom
[2] Department of Electronic and Electrical Engineering, University of Bath, BA2 7AY Bath, United Kingdom

E-mail: kl514@cam.ac.uk

Keywords: cathodoluminescence, point defects, core-shell nanorods, non-radiative recombination centres, hyperspectral mapping

Supplementary material for this article is available online

OPEN ACCESS

RECEIVED
13 December 2020

REVISED
16 February 2021

ACCEPTED FOR PUBLICATION
24 February 2021

PUBLISHED
8 March 2021

Abstract

Core-shell nanorod based light-emitting diodes (LEDs) with their exposed non-polar surfaces have the potential to overcome the limitations of planar LEDs by circumventing the quantum confined stark effect. In this experiment, InGaN/GaN core-shell nanorods were fabricated by a combination of top-down etching and bottom-up regrowth using metal-organic vapour phase epitaxy. When viewing the nanorods along their long axis, monochromatic cathodoluminescence maps taken at the GaN near-band-edge emission energy (3.39 eV) reveal a ring-like region of lower emission intensity. The diameter of this ring is found to be 530 (±20)nm corresponding to the ~510 nm diameter nickel etch masks used to produce the initial GaN nanopillars. Thus, the dark ring corresponds to the regrowth interface. To understand the origin of the ring, scanning transmission electron microscopy (STEM) and cathodoluminescence (CL) hyperspectral mapping at 10K were performed. STEM imaging reveals the absence of extended defects in the nanorods and indeed near the regrowth interface. Monochromatic CL maps recorded at 10K show that the ring remains dark for monochromatic maps taken at the GaN near-band-edge emission energy (3.47 eV) but is bright when considering the donor-acceptor pair emission energy (3.27 eV). This peculiar anticorrelation indicates that the dark ring originates from an agglomeration of point defects associated with donor-acceptor pair emission. The point defects are incorporated and buried at the GaN regrowth interface from the chemical and/or physical damage induced by etching and lower the radiative recombination rate; limiting the radiative efficiency close to the regrowth interface.

1. Introduction

Vertically-aligned radial core-shell nanorods have been shown to provide means to overcome the limitations of conventional planar quantum well (QW) LEDs based on wurtzite GaN [1–4]. The nanorods can be fabricated by two main methods being fully bottom-up and hybrid top-down/bottom-up approaches [1–4]. The hybrid approach, which will be the focus of this letter, provides advantages such as high uniformity of the nanorod array [5]. However, this method can suffer from defect incorporation through etch related damage [2, 6].

For GaN-based planar LEDs, the mature growth direction is the polar [0001] *c*-direction which is hampered by inherent spontaneous and piezoelectric polarisation fields leading to a reduced electron-hole overlap in the active region, limiting device efficiency [7]. This is known as the quantum-confined Stark effect (QCSE). GaN-based core-shell nanorod structures grown aligned to the [0001] direction possess accessible non-polar {10–10} *m*-plane facets. QWs grown on these non-polar facets are not affected by the detrimental effects of the QCSE which can potentially enhance LED device efficiency [8]. In addition, the nanorod geometry also provides a reduced dislocation density due to dislocation bending and termination [9, 10], a strain relaxed structure that

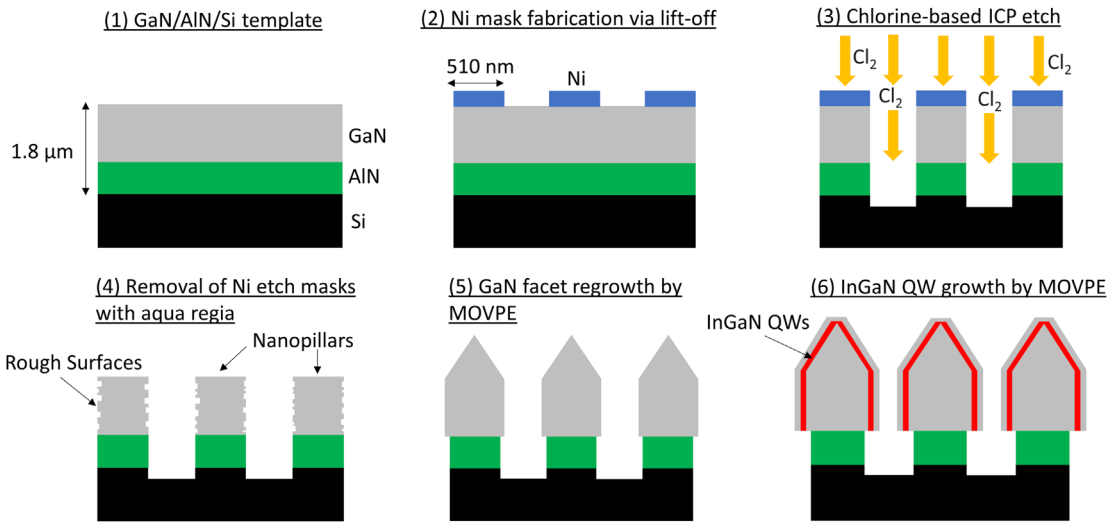

Figure 1. A step-by-step schematic illustrating the important steps in the fabrication of the nanorods. The fabrication steps proceed sequentially from (1) to (6).

limits stress build-up hindering crack nucleation [11], and a high surface-area-to-volume ratio which reduces carrier density in the QWs limiting the effects of efficiency droop [12].

However, as with their planar counterparts, core-shell nanostructures can suffer from structural defects such as stacking faults [13], point defects [14] and dislocations [15, 16]. These are known to deteriorate device performance by acting as non-radiative recombination centres competing with the desired radiative recombination channels and lowering the device internal quantum efficiency [17]. In addition to this, defects can also provide unwanted radiative pathways altering the colourimetric properties of the LEDs [18]. Thus, it is crucial to understand the origin and properties of these defects to control their incorporation and optimise the materials for their devices. One way to do this is to investigate the nanoscale relationship between the optical and structural properties of defect-containing nanorods. Cathodoluminescence (CL) hyperspectral imaging is suited for this investigation as it provides a nanoscale spatial resolution to probe localised variations in the optical properties of the nanorods. When coupled with other techniques (e.g scanning transmission electron microscopy (STEM)), the optical properties can then be correlated with the structural properties.

In this letter, CL is applied to investigate the origins of a circular region of lower emission intensity in InGaN/GaN core-shell nanorods fabricated by a combination of dry etching and regrowth.

2. Methods

The nanorods investigated were fabricated using a top-down/bottom-up hybrid approach. The nanopillars forming the GaN core were produced from a planar GaN/AlN/Si template grown by metal-organic vapour phase epitaxy (MOVPE). Firstly, a hexagonal array of circular nickel (Ni) metal masks was created on the GaN layer of the template via lift-off. The diameter of the masks was approximately 510 nm. Following this, the masked template was etched using chlorine-based inductively coupled plasma reactive-ion etching (ICP-RIE). Etching produced slightly tapered and rough GaN nanopillars. To recover smooth facets, GaN refacetting was performed in an MOVPE reactor using trimethylgallium (TMGa) and NH_3 as the precursors. After facet regrowth, 3 InGaN quantum wells (QWs) were grown on the nanorods with trimethylindium (TMIn), TMGa and NH_3 as precursors. The fabrication method is explained in more detail by Le Boulbar *et al* [16] and is shown schematically in figure 1.

Following growth, CL measurements were performed in an Attolight Allalin 4027 Chronos scanning electron microscope cathodoluminescence (SEM-CL) system at room temperature (RT) and at 10K by cooling the sample stage using liquid helium. At RT, measurements were taken using a beam current of 1 nA and an acceleration voltage of 5 kV which corresponds to 90% of the beam energy being deposited in a depth of ≈115 nm as determined using *Monte Carlo Casino* software [19]. At 10K, measurements were recorded using a beam current of 10 nA and an acceleration voltage of 3 kV corresponding to 90% of the beam energy being deposited in a depth of ≈56 nm. The CL hyperspectral maps were analysed using *Hyperspy* [20].

A radial cross-section from a nanorod was prepared using an FEI Helios focused ion beam (FIB) microscope by milling with a gallium ion beam operating at 30 kV. Firstly, the nanorod was sectioned and placed on an

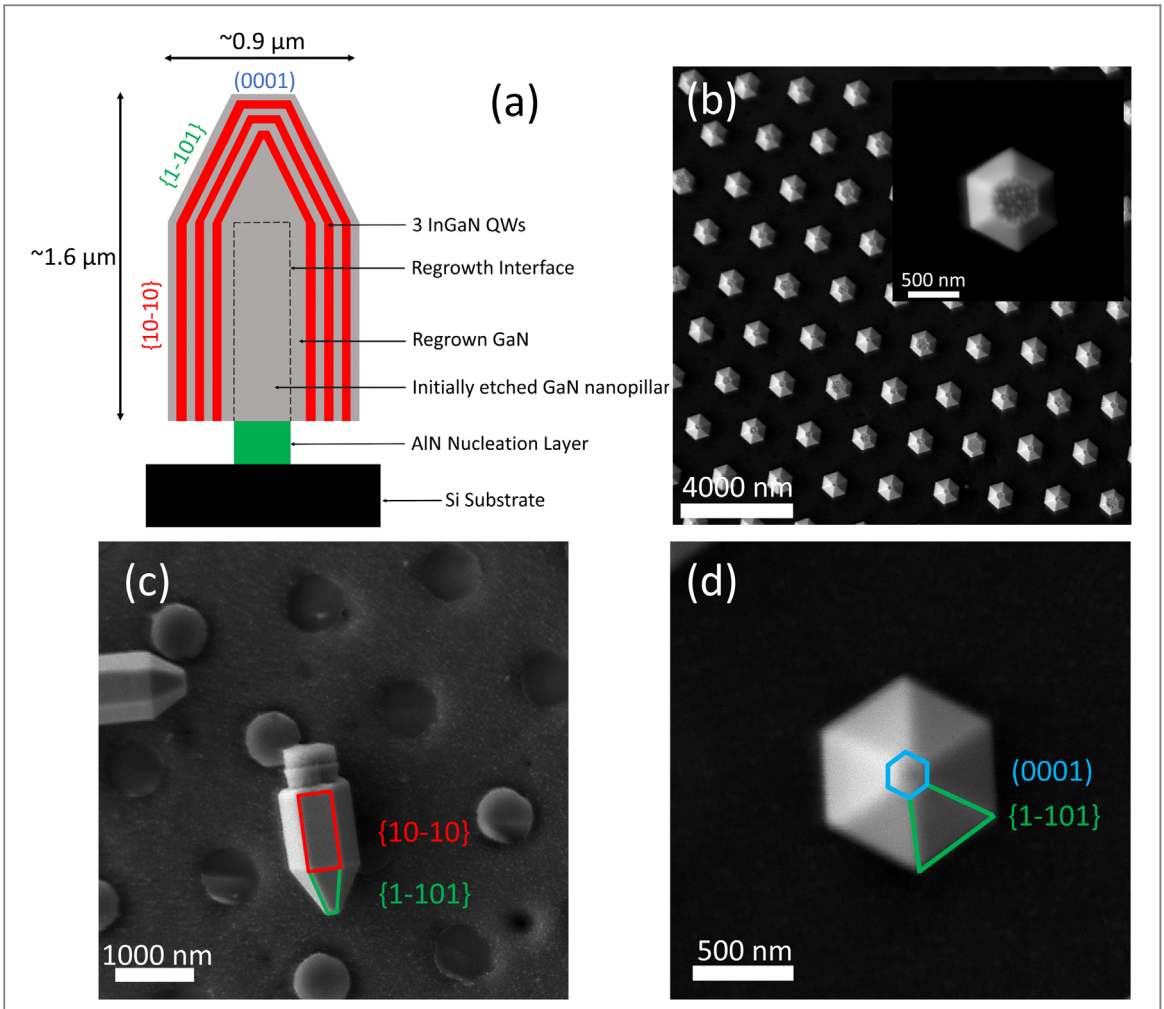

Figure 2. (a) Schematic representation of the core-shell nanorod heterostructure (drawn not to scale). The GaN etched nanopillar and regrown GaN are highlighted. (b) SE image of the InGaN/GaN core-shell nanorod array. The insert shows a nanorod that retained the (0001) *c*-plane facet. (c) and (d) highlight the top and side views of the nanorods along with the non-polar {10–10}, semi-polar {1–101}, and polar (0001) planes as represented by the coloured lines and labels.

EM-Tec 3 post Cu FIB lift-out grid adhered using a Pt source. Milling was performed from the tip of the nanorod towards the intersection of the semi-polar and non-polar planes achieving a lamella of thickness below 100 nm. The lamella was imaged using an FEI Osiris scanning transmission electron microscope (STEM) and high-angle annular dark-field (HAADF) images recorded. The microscope was operated at 200 kV with a beam current of 80 pA.

3. Results and discussion

The structure of a single nanorod is shown in figure 2(a) highlighting the GaN core nanopillar, regrown GaN and InGaN QW shells. The nanorods investigated in this work can be seen, from the top, as a uniform hexagonal array in the secondary electron (SE) image shown in figure 2(b). Figures 2(c) and (d) highlight the respective side and top views on a single nanorod. Note that the side view is that of a felled nanorod. From the SE images, it can be seen that each nanorod consists of six {10–10} non-polar *m*-plane side-walls which intersect with six {1–101} semi-polar facets that form the tip region of the nanorod (marked respectively as red and green in figure 2(c)). Most of the nanorods shown have retained a small polar (0001) *c*-plane facet at the apex of nanorod (marked as blue in figure 2(d)) and highlighted by the insert in figure 2(b). From the images, the average diameter and height of the nanorods were measured to be 850 (±50)nm and 1600 (±50)nm respectively.

To investigate the optical properties of the nanorods, CL imaging was performed at room temperature using an acceleration voltage of 5 kV and a beam current of 1 nA. Figure 3 shows the CL spectrum spatially averaged over the field of view depicted in figure 2(c). The mean CL spectrum shows that the emission intensity of the nanorods is dominated by an emission peak centred at 2.68 eV attributed to the InGaN QWs. A smaller peak centred at 3.39 eV corresponding to GaN near-band-edge (NBE) emission is also observed. It is noted here that

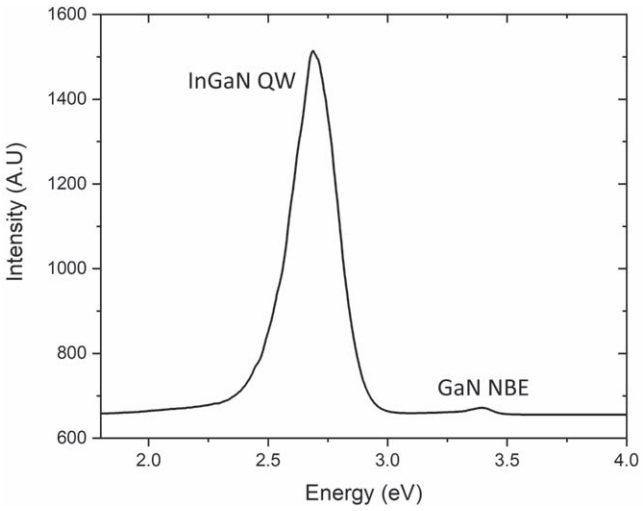

Figure 3. Shows the room temperature mean CL spectrum recorded from the field of view given in figure 2(c). The InGaN QW (2.68 eV) and GaN NBE (3.39 eV) emission peaks can be observed.

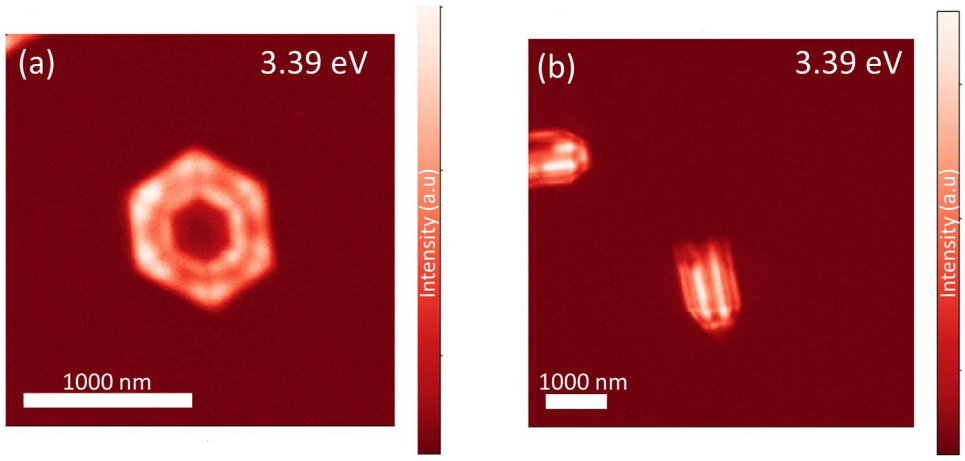

Figure 4. (a) and (b) Show monochromatic CL maps of the nanorods as viewed from the top and side respectively and at a photon energy of 3.39 eV.

no significant changes in the mean spectrum are observed when considering a larger area of the wafer. This is shown by figure S1 in the supplementary information.

To reveal the spatial variation of the GaN NBE (3.39 eV) luminescence, we extracted monochromatic maps from the hyperspectral datasets by applying a digital bandpass filter. The maps are shown in figures 4(a) and (b) for the nanorods in figures 2(d) and (c) respectively. The top view monochromatic map shows a ring of lower emission intensity compared to the regions that border it. Surrounded by the ring is a dark central region that corresponds to the *c*-plane facet. The central region is darker due to a lower crystalline quality as evidenced by the rough and serrated surface, visible in the insert of figure 2(b), likely strongly enhancing the incorporation of point defects. The inner diameter of the lower intensity ring was calculated to be 530 (±20)nm which is similar to the ~510 nm diameter nickel masks used to produce the GaN nanopillars by ICP-RIE. Thus, the position of the ring corresponds to the regrowth interface or near-surface region of the nanopillars. The lower emission intensity region can be seen to extend from the ring towards the middle regions of the *m*-plane side-walls with the apexes between *m*-planes being brightest. Brighter apexes and darker middle regions of the side-walls can also be observed in the side view monochromatic map which implies that the pattern persists throughout the length of the nanorod.

In order to resolve the origins of this lower intensity pattern we will consider several possibilities; the presence of extended defects, optical modes inside the nanorod cavity and point defect agglomeration.

Extended defects such as dislocations and stacking faults can locally lower the emission intensity by acting as non-radiative recombination centres [21, 22]. To investigate the presence of extended defects, STEM-HAADF

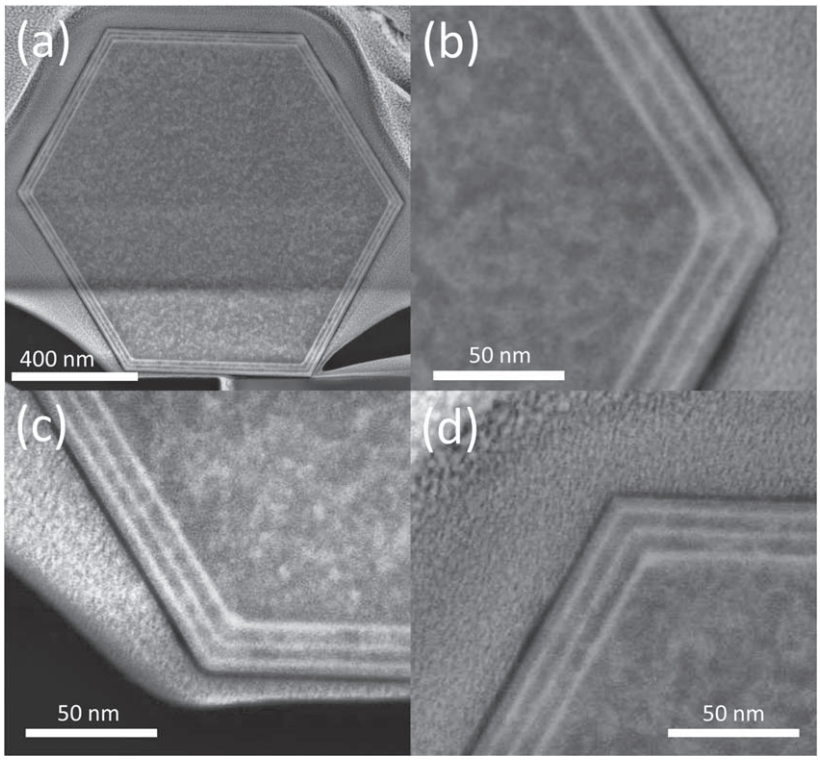

Figure 5. STEM-HAADF images of a FIB milled nanorod taken using an acceleration voltage of 200 kV. (a) Shows the cross-section analysed while (b)–(d) highlights three ridge regions of the milled nanorod cross-section.

images were recorded on a FIB milled nanorod and are shown in figure 5. In figures 5(a)–(d), no extended defects can be observed at the regrowth interface or at any other region on the nanorods. In fact, the interface between the GaN etched nanopillar and the regrowth is seamless, with no visible contrast. This lack of extended defects is supported by literature data on similar nanorods. Here, extended defects such as stacking faults are reported as absent from the regrowth interface while threading dislocations are known to bend and terminate at the lower regions of the nanorods thus having little effect on the spatial distribution of luminescence [1, 12, 15, 16, 23].

Optical modes can also arise in hexagonal GaN nanorods and may play a part in producing the intensity pattern we observe [24–26]. The optical modes usually appear as whispering gallery or Fabry-Pérot resonances in hexagonal nanorods or disks [24, 26]. These can form optical structures in the nanorods which affect the observed spatial distribution of light emission [26–28]. Such optical structures can rationalise the pattern observed in figure 4. Considering the panchromatic map given in figure 6(a), no optical structures can be observed. This may indicate that the lower intensity pattern is not a result of optical modes. On the other hand, the observation may also show how side-wall QW luminescence dominates the emission intensity obscuring other intensity variations in the panchromatic map.

A CL spot-spectrum in the region where the lower intensity ring is observed (green dot in figure 6(a)) is displayed in figure 6(b). The spot-spectrum shows regular repeating peaks that are superimposed onto the QW luminescence peak. The regularity of the peaks might suggest that they relate to optical modes [24–26, 29]. But these peaks do not appear towards the right of the QW luminescence peak nor on the GaN NBE peak. In addition to this, their common spacing of approximately 90 meV indicates that they are instead longitudinal optical (LO) phonon replicas [30, 31]. Nonetheless, from the data collected, it is difficult to say with any certainty that the lower intensity pattern is due to optical modes or not. CL experiments on partial nanorod structures which would not be expected to exhibit optical modes[14] are planned in future with the aim of eliminating this possibility.

The most likely candidate for the origin of the lower intensity pattern are point defects. To investigate the presence of point defects, CL hyperspectral imaging was performed at 10K using a primary beam energy of 3 keV and a 10 nA beam current. Figure 7(a) shows the mean CL spectrum spatially averaged over the field of view in (b). At 10K, two emission bands are observed on the higher energy side of the InGaN QW peak, which is centred at 2.77 eV. The first band, centred at 3.47 eV, is attributed to emission from GaN NBE [32]. The second luminescence band comprises of two peaks at 3.27 eV and 3.18 eV with a shoulder at 3.08 eV. This band is assigned to donor-acceptor pair (DAP) luminescence which usually consists of a zero-phonon peak near 3.27 eV followed by LO phonon replicas at lower energies [32]. As such, the peak centred at 3.27 eV is taken to be the

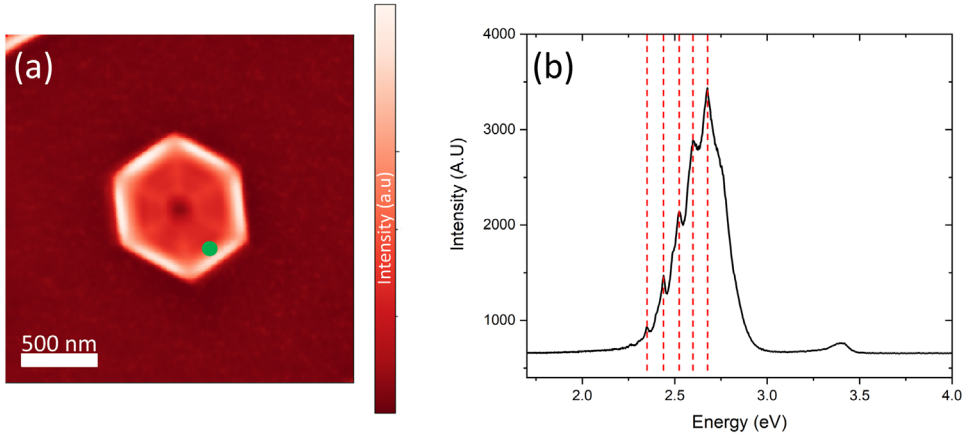

Figure 6. (a) Shows a panchromatic CL image of nanorod luminescence and the position (green dot) on the nanorod where the spot spectrum shown in (b) was extracted.

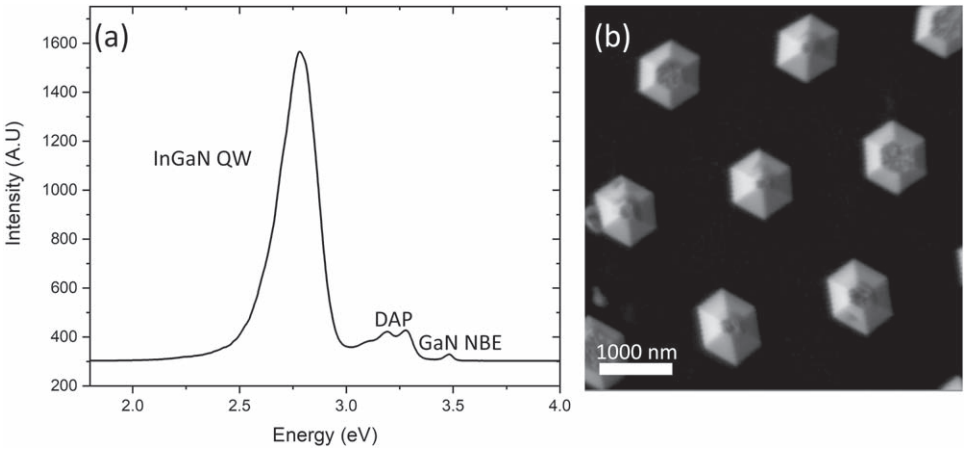

Figure 7. (a) The mean CL spectrum recorded at 10K from the field of view given by the SE image in (b). The GaN NBE and donor-acceptor pair (DAP) emission bands are shown.

zero-phonon peak while those at 3.18 eV and 3.08 eV are the first and second LO phonon replicas [32]. This assignment is supported by the regular spacing of approximately 100 meV, found between adjacent peaks, which is in good agreement with 91 meV reported in the literature for the LO phonon spacing in GaN [30, 33].

Monochromatic CL maps at the peaks observed in figure 7(a) are shown in figures 8(a)–(b). Comparing figures 8(a) to (b), a peculiar anti-correlation in the emission intensity can be observed in the region near the regrowth interface. The intensity within this region remains lower when considering GaN NBE emission at 3.47 eV. However, for the DAP-related monochromatic CL map (3.27 eV), the region is brighter than the surroundings. This phenomenon is highlighted by the juxtaposition of figures 8(c) and (d) which highlight the nanorod marked by the white square. It can be observed that the dashed loop, which traces the region of the dark ring in figure 8(c), maps onto a bright ring in (d). Additional evidence that these phenomena are occurring around the same region is provided by their diameters. The diameter of the brighter ring, defined as half the sum of the apparent inner and outer diameters, was found to be 520($\pm$20)nm. This is in good agreement with the 530($\pm$20)nm calculated for the dark ring in the room temperature data.

Given that DAP emission is related to acceptor and donor-like point defects such as silicon, oxygen, carbon and gallium vacancies [32, 34]. It follows that the dark ring originates from an agglomeration of point defects. Since the ring pattern has been established to correlate with the near-surface region of the nanopillars, it can be inferred that the dark ring originates from etch-induced damage. ICP-RIE has been reported to cause physical and chemical damage to GaN through ion bombardment [6, 35]. Ion bombardment can induce point defects in the GaN etched nanopillars such as N vacancies and Ga vacancy complexes [6, 36]. The literature suggests that the prominent point defects induced by physical etching of GaN are nitrogen vacancies because N atoms are preferentially removed over Ga atoms [37–39]. Preferential etching creates a Ga rich surface. By utilising

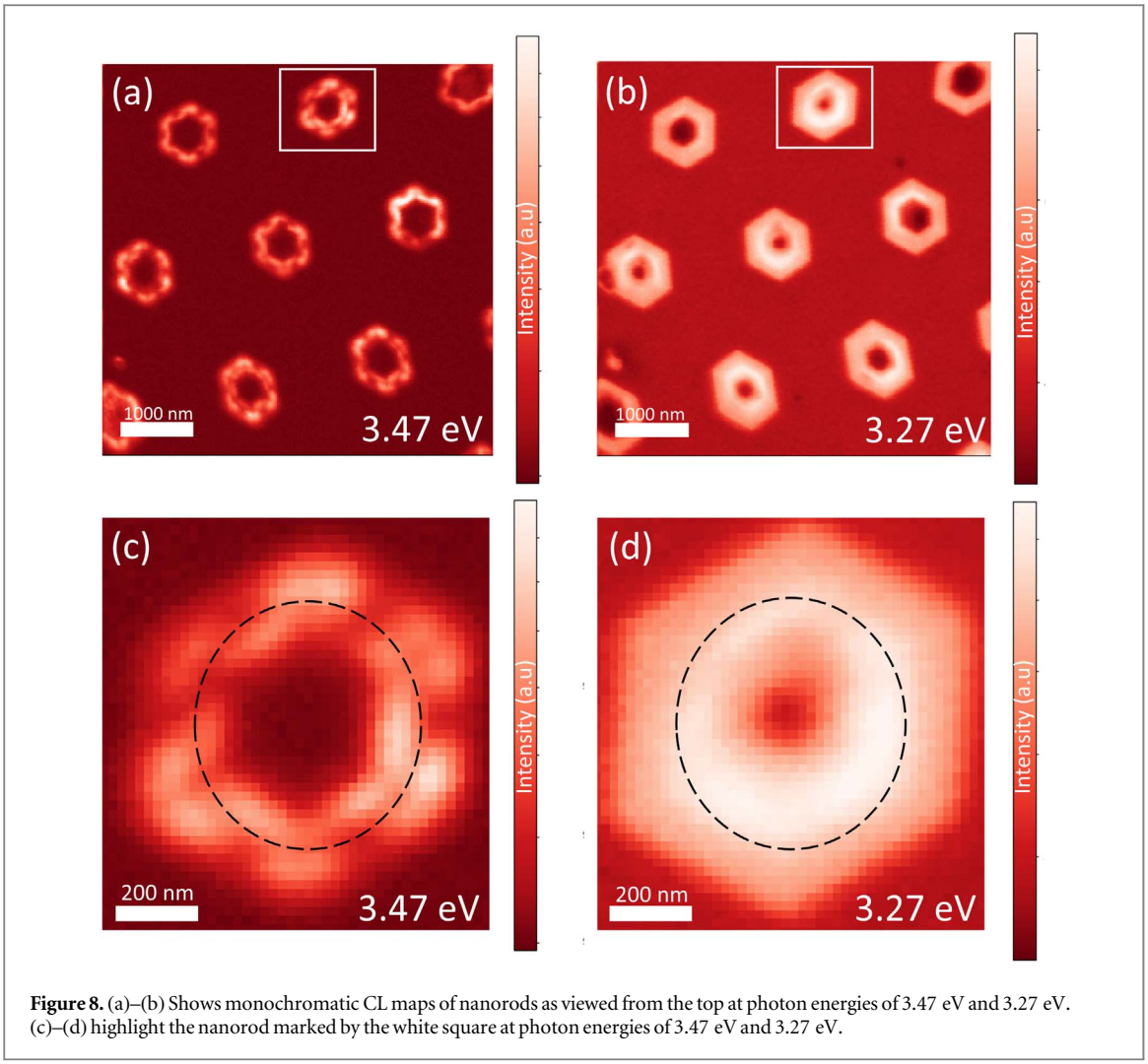

Figure 8. (a)–(b) Shows monochromatic CL maps of nanorods as viewed from the top at photon energies of 3.47 eV and 3.27 eV. (c)–(d) highlight the nanorod marked by the white square at photon energies of 3.47 eV and 3.27 eV.

secondary-ion-mass spectroscopy, Lin *et al* found the thickness of this Ga-rich top-layer to be ~60 nm [6]. This is in good agreement with the value of 60 (±10)nm measured for the thickness of the dark ring using room temperature data. In addition to nitrogen vacancies, etch damage can also create dangling bonds on the GaN nanopillar surface. Dangling bonds can enhance adsorption of impurities such as environmental oxygen, creating non-native point defects [36, 37]. Thus, point defects in the region near the regrowth interface lower the observed GaN NBE emission intensity which manifests as the dark ring.

To reduce the concentration of point defects at the regrowth interface, a potassium hydroxide (KOH) wet etching step is usually employed to strip away the ICP-RIE damaged outer layer of the nanopillars before regrowth [40]. However, KOH would have selectively attacked the silicon substrate in this case and could not be employed [41, 42]. Thermal annealing has also been shown to alleviate surface deformities after ICP-RIE etching and could have helped prevent the point defect accumulation observed [43].

The increase in point defect concentration has been observed in the literature to correlate with a reduction in the internal quantum efficiency of InGaN/GaN LEDs [44]. This is possibly due to the point defects acting as deep level traps in the band-gap which act as non-radiative recombination centres [44]. In our study, only a few nanorods from one sample were investigated. It is thus difficult to say how the point defects at the interface will affect the performance of the nanorods as LEDs. However, the presence of point defects at the regrowth interface does not appear to impact the emission properties of the InGaN QWs as no drop in intensity is observed in figure 6(a). This is perhaps on account of the region of point defect agglomeration not encroaching on the QWs as the GaN regrowth is sufficiently thick. Similar effects have observed for InGaN underlayers (UL) and GaN spacers in InGaN/GaN QWs. The UL and spacer layers have been observed to prevent degradation of the QWs that would otherwise be induced by their growth on a defected GaN surface [45, 46]. This results in an improved QW radiative efficiency. An investigation performed on similar nanorods with various regrowth times and hence GaN regrowth thickness could help quantify the impact of point defects on the emission characteristics of the QWs. Despite this, the GaN core is likely to be the n or p-doped layer of a grown device, as such, an interface with a high point defect concentration may still be detrimental to device operation.

4. Conclusions

InGaN/GaN core-shell nanorods prepared by a top-down etching and bottom-up facet regrowth process were investigated using CL hyperspectral and STEM-HAADF imaging. From monochromatic CL maps at 3.39 eV (GaN NBE emission), a ring-like region of lower emission intensity was observed and was found to correspond to the regrowth interface. STEM-HAADF images from a FIB milled lamella reveal no extended defects in the nanorod with the regrowth interface being seamless showing no difference in contrast. Optical resonance modes may contribute to the low intensity region observed, however, this is unlikely. It is most likely that the dark ring originates from point defects incorporated by physical and/or chemical etch damage of the GaN etched nanopillars. These can be nitrogen vacancies from the preferential etching of nitrogen or adsorbed environmental oxygen enhanced by the creation of dangling bonds. Evidence of point defects is provided by an observed anticorrelation of emission intensity in the region of the ring when juxtaposing GaN NBE and DAP monochromatic CL maps at 10 K. The DAP monochromatic map shows a bright ring while the ring is dark in the GaN NBE map. Thus, point defect agglomeration near the regrowth interface gives rise to an increased non-radiative recombination rate producing the dark ring observed. As the point defects are localised near the regrowth interface, they are observed to have no influence on the emission properties of the QWs. However, a high point defect concentration at the interface may still be detrimental to device operation.

Acknowledgments

This research was supported by the EPSRC under grant numbers EP/R025193/1 and EP/M015181/1, 'Manufacturing nano-engineered III-nitrides'. K Loeto would like to acknowledge the Botswana government for his Ph.D funding. Dr Christian Monachon of Attolight is thanked for his ongoing support of the system.

Data availability statement

All data that support the findings of this study are included within the article (and any supplementary files).

ORCID iDs

K Loeto https://orcid.org/0000-0002-1694-2102
G Kusch https://orcid.org/0000-0003-2743-1022
SM Fairclough https://orcid.org/0000-0003-3781-8212

References

[1] Gwo S, Lu Y, Lin H, Kuo C, Wu C, Lu M and Chen L 2017 Chapter ten—nitride semiconductor nanorod heterostructures for full-color and white-light applications *Semiconductors and Semimetals* 96 (Amsterdam: Elsevier) 10 341–84
[2] Li S and Waag A 2012 GaN based nanorods for solid state lighting *J. Appl. Phys.* **111** 071101
[3] Kang M S, Lee C-H, Park J B, Yoo H and Yi G-C 2012 Gallium nitride nanostructures for light-emitting diode applications *Nano Energy* **1** 391–400
[4] Zhao S, Nguyen H P, Kibria M G and Mi Z 2015 III-Nitride nanowire optoelectronics *Prog. Quantum Electron.* **44** 14–68
[5] Le Boulbar E D, Gîrgel I, Lewins C J, Edwards P R, Martin R W, Šatka A, Allsopp D W E and Shields P A 2013 Facet recovery and light emission from GaN/InGaN/GaN core-shell structures grown by metal organic vapour phase epitaxy on etched GaN nanorod arrays *J. Appl. Phys.* **114** 094302
[6] Lin Y-J and Chu Y-L 2005 Effect of reactive ion etching-induced defects on the surface band bending of heavily Mg-doped p-type GaN *J. Appl. Phys.* **97** 104904
[7] Kaplar R, Kurtz S and Koleske D 2005 Quantum-confined stark effect and polarization field in single quantum well InGaN/GaN LEDs *MRS Proceedings* **892** 0892–FF32-01
[8] Waltereit P, Brandt O, Trampert A, Grahn H T, Menniger J, Ramsteiner M, Reiche M and Ploog K H 1919 Nitride semiconductors free of electrostatic fields for efficient white light-emitting diodes *Nature* **406** 865–8
[9] Wang G T, Li Q, Wierer J J, Koleske D D and Figiel J J 2014 Top-down fabrication and characterization of axial and radial III-nitride nanowire LEDs *Physica Status Solidi (a)* **211** 748–51
[10] Coulon P M, Mexis M, Teisseire M, Jublot M, Vennéguès P, Leroux M and Zuniga-Perez J 2014 Dual-polarity GaN micropillars grown by metalorganic vapour phase epitaxy: Cross-correlation between structural and optical properties *J. Appl. Phys.* **115** 153504
[11] Kawakami Y, Suzuki S, Kaneta A, Funato M, Kikuchi A and Kishino K 2006 Origin of high oscillator strength in green-emitting InGaN-GaN nanocolumns *Appl. Phys. Lett.* **89** 163124
[12] Griffiths J T *et al* 2017 Structural impact on the nanoscale optical properties of InGaN core-shell nanorods *Appl. Phys. Lett.* **110** 172105
[13] Robin Y *et al* 2019 Localization and transient emission properties in InGaN/GaN quantum wells of different polarities within core-shell nanorods *Nanoscale* **11** 193–9
[14] Zhao B, Lockrey M N, Wang N, Caroff P, Yuan X, Li L, Wong-Leung J, Tan H H and Jagadish C 2020 Highly regular rosette-shaped cathodoluminescence in GaN self-assembled nanodisks and nanorods *Nano Res.* **13** 2500–5

[15] Gîrgel I, Edwards P R, Le Boulbar E, Coulon P-M, Sahonta S L, Allsopp D W E, Martin R W, Humphreys C J and Shields P A 2016 Investigation of indium gallium nitride facet-dependent nonpolar growth rates and composition for core-shell light-emitting diodes *J. Nanophotonics* **10** 1–11
[16] Le Boulbar E D *et al* 2016 Structural and optical emission uniformity of m-plane InGaN single quantum wells in core-shell nanorods *Crystal Growth & Design* **16** 1907–16
[17] Chang C, Chen L, Huang L, Wang Y, Lu T and Huang J J 2012 Effects of strains and defects on the internal quantum efficiency of InGaN/GaN nanorod light emitting diodes *IEEE J. Quantum Electron.* **48** 551–6
[18] Medvedev O, Vyvenko O, Ubyivovk E, Shapenkov S, Bondarenko A, Saring P and Seibt M 2018 Intrinsic luminescence and core structure of freshly introduced a-screw dislocations in n-GaN *J. Appl. Phys.* **123** 161427
[19] Drouin D, Couture A R, Joly D, Tastet X, Aimez V and Gauvin R 2007 CASINO V2.42-A fast and easy-to-use modeling tool for scanning electron microscopy and microanalysis users *Scanning* **29** 92–101
[20] Peña F D L *et al* 2018 hyperspy/hyperspy v1.4.1 (Version v1.4.1) (https://doi.org/10.5281/zenodo.3396791)
[21] Naresh-Kumar G *et al* 2014 Coincident electron channeling and cathodoluminescence studies of threading dislocations in GaN *Microsc. Microanal.* **20** 55–60
[22] Kusch G *et al* 2015 Spatial clustering of defect luminescence centers in Si-doped low resistivity Al0.82Ga0.18N *Appl. Phys. Lett.* **107** 072103
[23] Chen H-Y, Lin H-W, Shen C-H and Gwo S 2006 Structure and photoluminescence properties of epitaxially oriented GaN nanorods grown on Si(111) by plasma-assisted molecular-beam epitaxy *Appl. Phys. Lett.* **89** 243105
[24] Coulon P-M, Hugues M, Alloing B, Beraudo E, Leroux M and Zuniga-Perez J 2012 GaN microwires as optical microcavities: whispering gallery modes Vs fabry-perot modes *Opt. Express* **20** 18707–16
[25] Tessarek C, Heilmann M and Christiansen S 2014 Whispering gallery modes in GaN microdisks, microrods and nanorods grown by MOVPE *Phys. Status Solidi* C **11** 794–7
[26] Kusch G, Conroy M, Li H, Edwards P R, Zhao C, Ooi B S, Pugh J, Cryan M J, Parbrook P J and Martin R W 2018 Multi-wavelength emission from a single InGaN/GaN nanorod analyzed by cathodoluminescence hyperspectral imaging *Sci. Rep.* **8** 1742
[27] Gong S-H, Ko S-M, Jang M-H and Cho Y-H 2015 Giant rabi splitting of whispering gallery polaritons in GaN/InGaN core-shell wire *Nano Lett.* **15** 4517–24
[28] Coulon P M *et al* 2017 Optical properties and resonant cavity modes in axial InGaN/GaN nanotube microcavities *Opt. Express* **25** 28246–57
[29] Tessarek C, Dieker C, Spiecker E and Christiansen S 2013 Growth of GaN nanorods and wires and spectral tuning of whispering gallery modes in tapered GaN wires *Japan. J. Appl. Phys.* **52** 08JE09
[30] Xu J, Chen L, Yu L, Liang H, Zhang B L and Lau K M 2007 Temperature dependence of cathodoluminescence spectra and stress analysis of a GaN layer grown on a mesa structured Si substrate *Journal of Applied Physics* **102** 104508-104508
[31] Capasso F and Cho A Y 1994 Bandgap engineering of semiconductor heterostructures by molecular beam epitaxy: physics and applications *Surf. Sci.* **299-300** 878–91
[32] Reshchikov M A and Morkoç H 2005 Luminescence properties of defects in GaN *J. Appl. Phys.* **97** 061301
[33] Paskova T, Arnaudov B, Paskov P P, Goldys E M, Hautakangas S, Saarinen K, Södervall U and Monemar B 2005 Donor-acceptor pair emission enhancement in mass-transport-grown GaN *J. Appl. Phys.* **98** 033508
[34] Ren G, Dewsnip D, Lacklison D, Orton J, Cheng T and Foxon C 1997 Donor acceptor pair in molecular beam epitaxy grown GaN *Materials Science and Engineering:* B **43** 242–5
[35] Lan W-H, Huang K-C, Huang K F, Lin J-C, Cheng Y-C and Lin W-J 2008 Annealing of defect states in reactive ion etched GaN *Proceedings of the 2nd International Symposium on Point Defect and Non-Stoichiometry (ISPN-2)* **69** 719–23
[36] Fan Q, Chevtchenko S, Ni X, Cho S-J and Morko H 2006 Recovery of GaN surface after reactive ion etching *Proc. SPIE* 6121
[37] Choi H W, Chua S J, Raman A, Pan J S and Wee A T S 2000 Plasma-induced damage to n-type GaN *Appl. Phys. Lett.* **77** 1795–7
[38] Li Q, Westlake K R, Crawford M H, Lee S R, Koleske D D, Figiel J J, Cross K C, Fathololoumi S, Mi Z and Wang G T 2011 Optical performance of top-down fabricated InGaN/GaN nanorod light emitting diode arrays *Opt. Express* **19** 25528–34
[39] Fan Z, Mohammad S N, Kim W, Aktas Z, Botchkarev A E and Morkoç H 1996 Very low resistance multilayer Ohmic contact to n-GaN *Appl. Phys. Lett.* **68** 1672–4
[40] Liu G, Wen B, Xie T, Castillo A, Ha J-Y, Sullivan N, Debnath R, Davydov A, Peckerar M and Motayed A 2015 Top-down fabrication of horizontally-aligned gallium nitride nanowire arrays for sensor development *Microelectron. Eng.* **142** 58–63
[41] Nguyen Q D and Elwenspoek M 2006 Characterisation of anisotropic etching in KOH using network etch rate function model: influence of an applied potential in terms of microscopic properties *J. Phys. Conf. Ser.* **34** 1038–43
[42] Zubel I and Kramkowska M 2004 Etch rates and morphology of silicon (h k l) surfaces etched in KOH and KOH saturated with isopropanol solutions *The 17th European Conference on Solid-State Transducers* **115** 549–56
[43] Conroy M *et al* 2016 Self-healing thermal annealing: surface morphological restructuring control of GaN nanorods *Crystal Growth & Design* **16** 6769–75
[44] Lee I-H, Polyakov A Y, Smirnov N B, Shchemerov I V, Lagov P B, Zinov'ev R A, Yakimov E B, Shcherbachev K D and Pearton S J 2017 Point defects controlling non-radiative recombination in GaN blue light emitting diodes: insights from radiation damage experiments *J. Appl. Phys.* **122** 115704
[45] Haller C, Carlin J-F, Jacopin G, Martin D, Butté R and Grandjean N 2017 Burying non-radiative defects in InGaN underlayer to increase InGaN/GaN quantum well efficiency *Appl. Phys. Lett.* **111** 262101
[46] Kapoor A, Finot S, Grenier V, Robin E, Bougerol C, Bleuse J, Jacopin G, Eymery J and Durand C 1919 Role of underlayer for efficient core-shell InGaN QWs grown on m-plane GaN wire sidewalls *ACS Appl. Mater. Interfaces* **12** 19092–101